

1

2 **Supplementary Information for**

3 **scMerge leverages factor analysis, stable expression, and pseudoreplication to merge**
4 **multiple single-cell RNA-seq datasets**

5 **Yingxin Lin, Shila Ghazanfar, Kevin Y. X. Wang, Johann A. Gagnon-Bartsch, Kitty K. Lo, Xianbin Su, Ze-Guang Han, John T.**
6 **Ormerod, Terence P. Speed, Pengyi Yang and Jean Yee Hwa Yang**

7 **Jean Yee Hwa Yang, Pengyi Yang**

8 **E-mail: J.Y.H.Y. jean.yang@sydney.edu.au and P.Y. pengyi.yang@sydney.edu.au**

9 **This PDF file includes:**

- 10 Figs. S1 to S17
- 11 Tables S1 to S2
- 12 Captions for Databases S1 to S2

13 **Other supplementary materials for this manuscript include the following:**

- 14 Databases S1 to S2

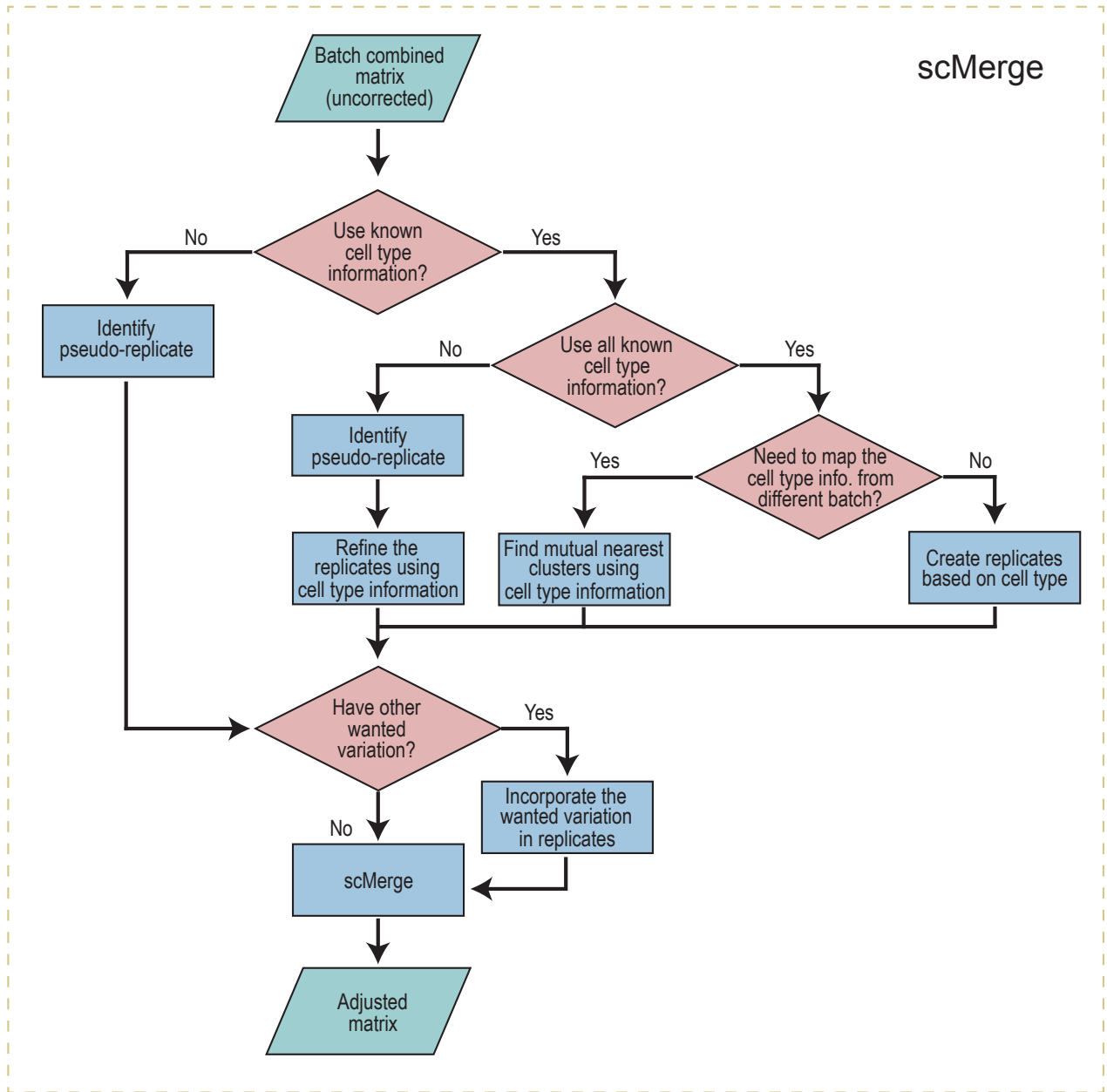


Fig. S1. Flow chart illustrating the decision-making process associated with scMerge algorithm.

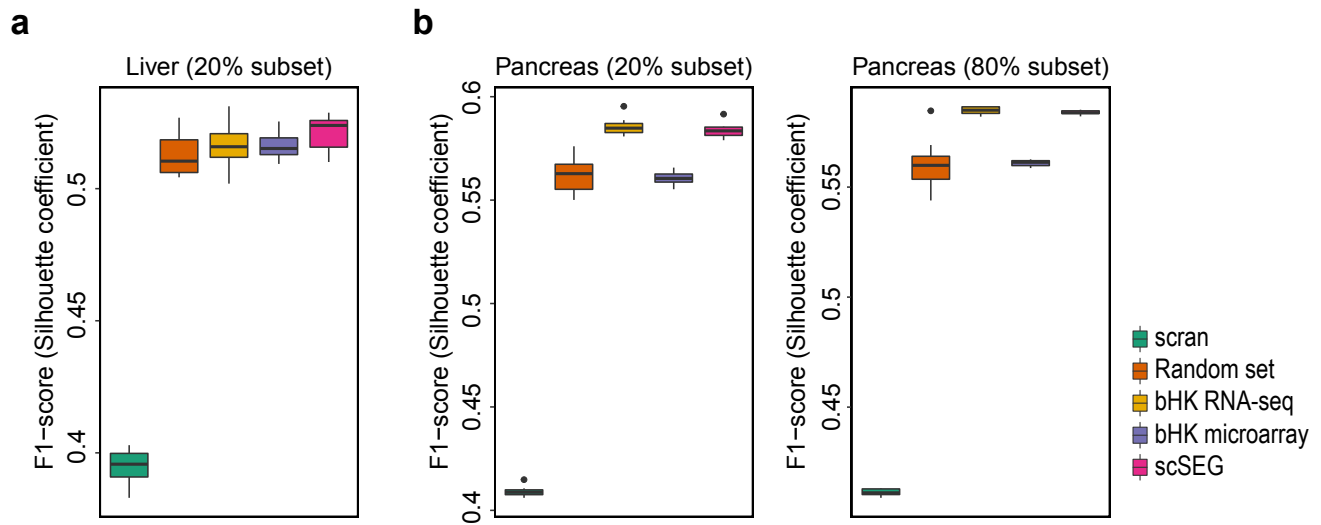


Fig. S2. A 1 by 3 panel of boxplots comparing the effect of different types of negative controls for (a) liver datasets and (b) four Pancreas datasets. The y-axis represents the F1 score of Silhouette coefficients between cell type mixing and (1 - datasets mixing). Stratified sampling is performed to randomly subset 20% and 80% of cells from the datasets. This procedure is repeated 10 times. The boxplots represent the F1 score results using logcounts, RUVg using random subset of genes, bulk microarray, RNA-Seq data, and scSEG as negative control genes based on subset of the datasets.

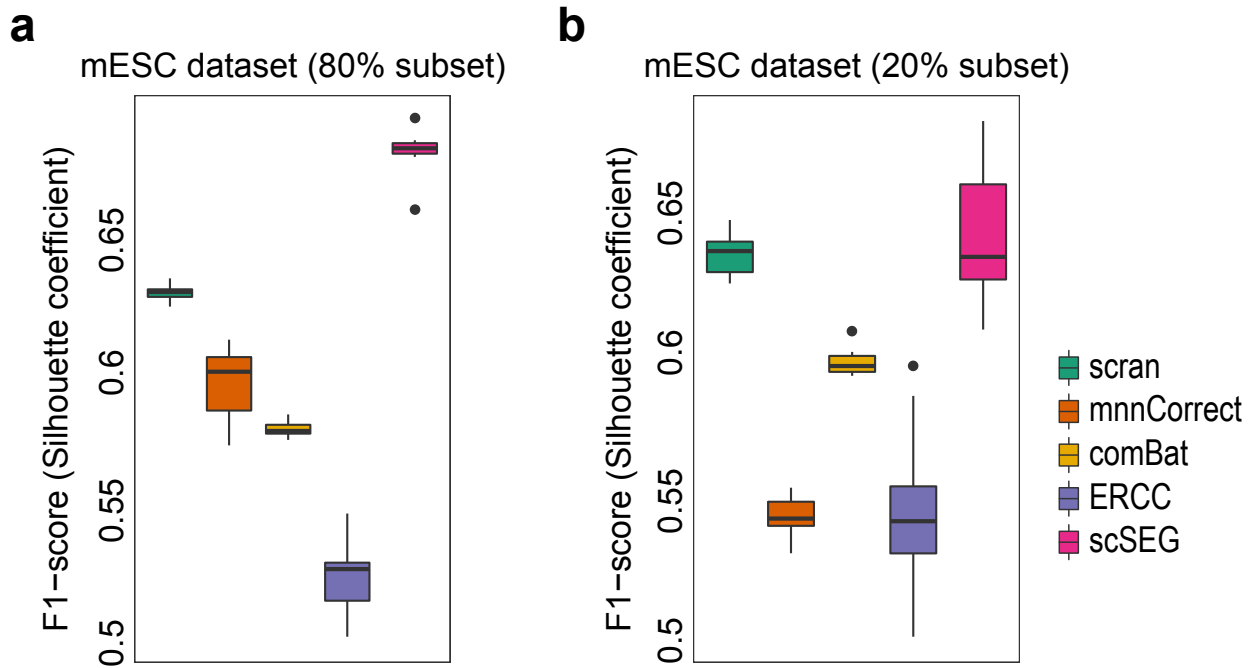


Fig. S3. A 1 by 2 panel of boxplots showing the effect of using ERCC and scSEG as negative controls with scMerge. Stratified subsampling is performed for the mESC dataset. In each stratified subsampling, we randomly selected 20% (left panel) or 80% (right panel) of the cells from the dataset and perform scMerge with ERCC spike-ins genes and mouse scSEG, and comparing the results with ComBat and mnnCorrect (default settings). This procedure is repeated 10 times.

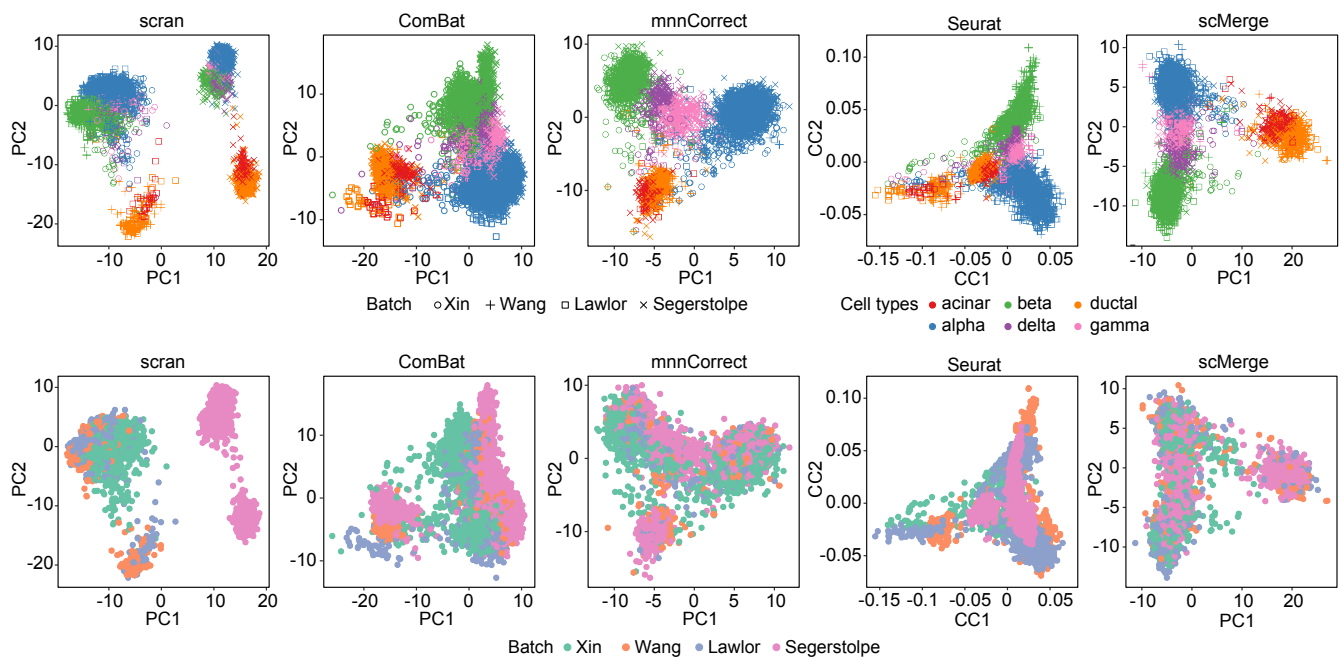


Fig. S4. A 2 by 5 panel of PCA plots of the four Pancreas datasets using the output from scrn (logcounts), ComBat, mnnCorrect, Seurat, and scMerge (using scSEG as negative controls). The top row of the panel is color coded by cell types and the second row is color coded by the four different datasets.

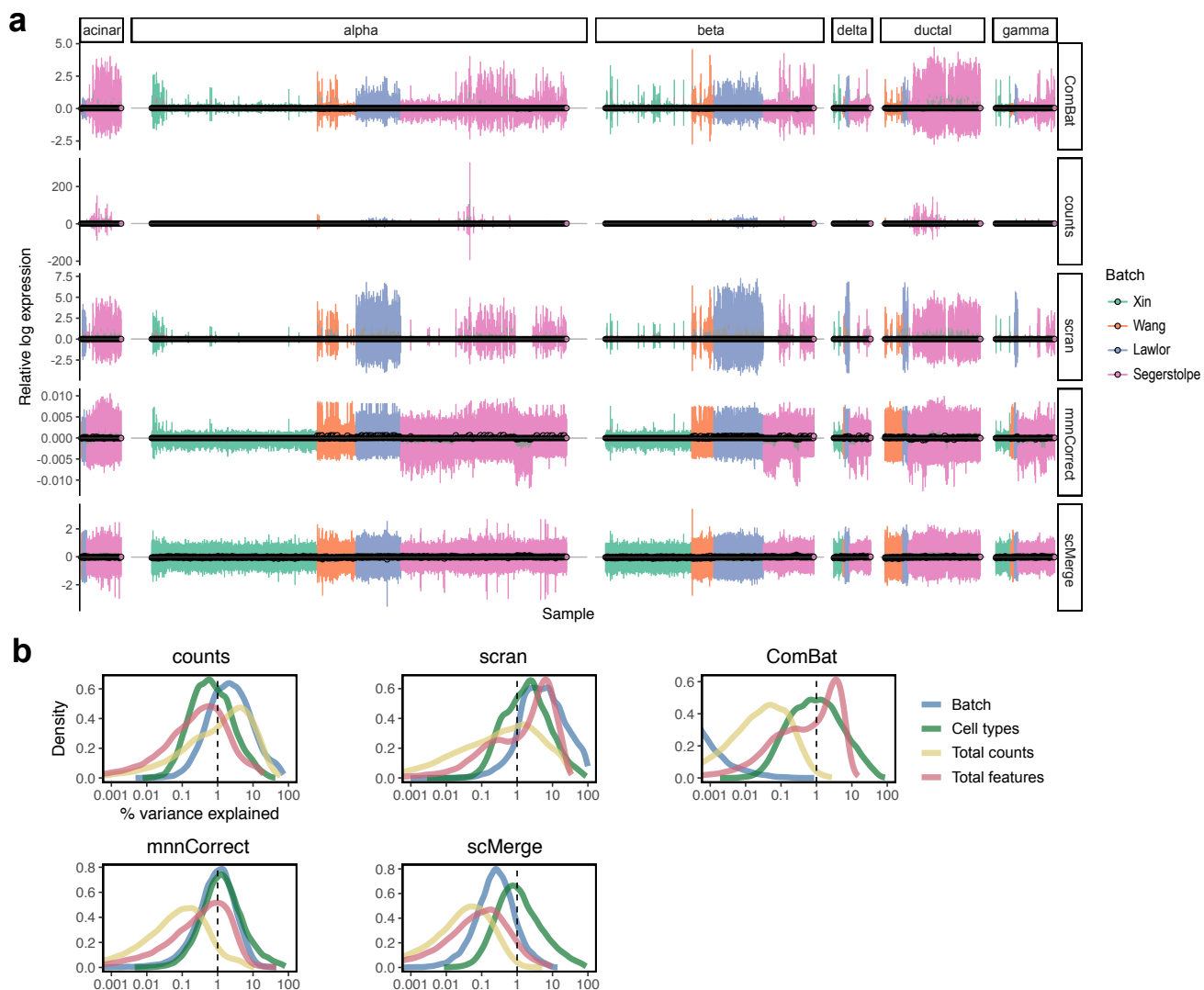


Fig. S5. Diagnostic plots from the Pancreas data collections (“Pancreas4”). A. RLE plots. The boxplot for each cell from the same cell type between different batches of scMerge shares similar inter quantile ranges. B. Percentage of variance explained for each variable. scMerge has cellType explaining the highest percentage of variation for the liver data collection.

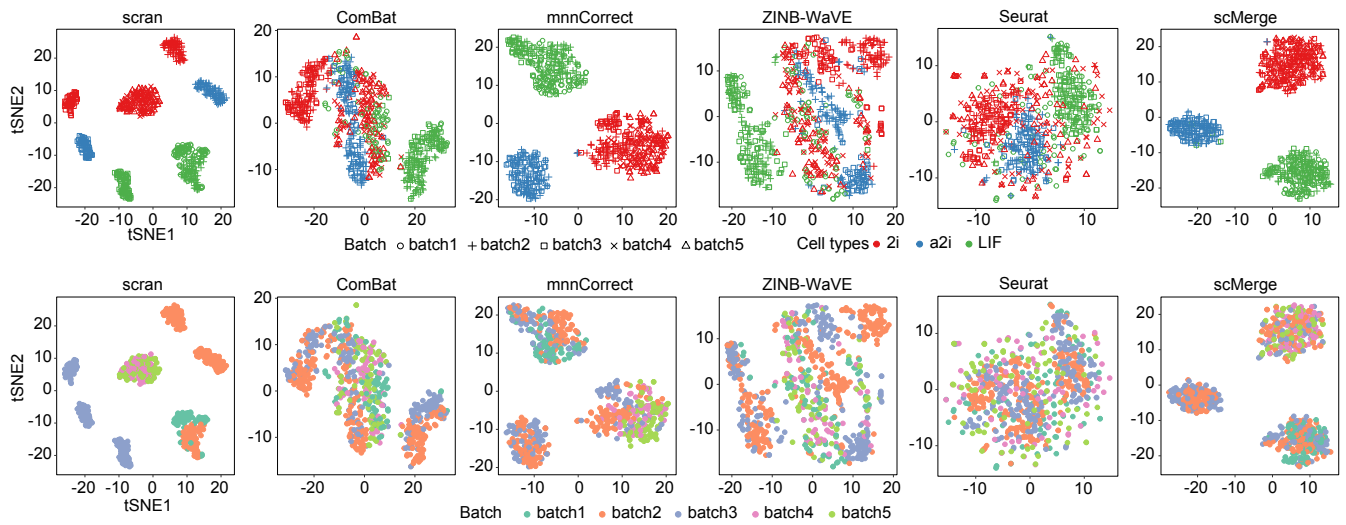


Fig. S6. A 2 by 6 panel of tSNE plots of the mESC datasets using the output from scran (logcounts), ComBat, mnnCorrect, ZINB-WaVE, Seurat, and scMerge (using scSEG as negative controls). The top row of the panel is color coded by three cell types and the second row is color coded by the three batches.

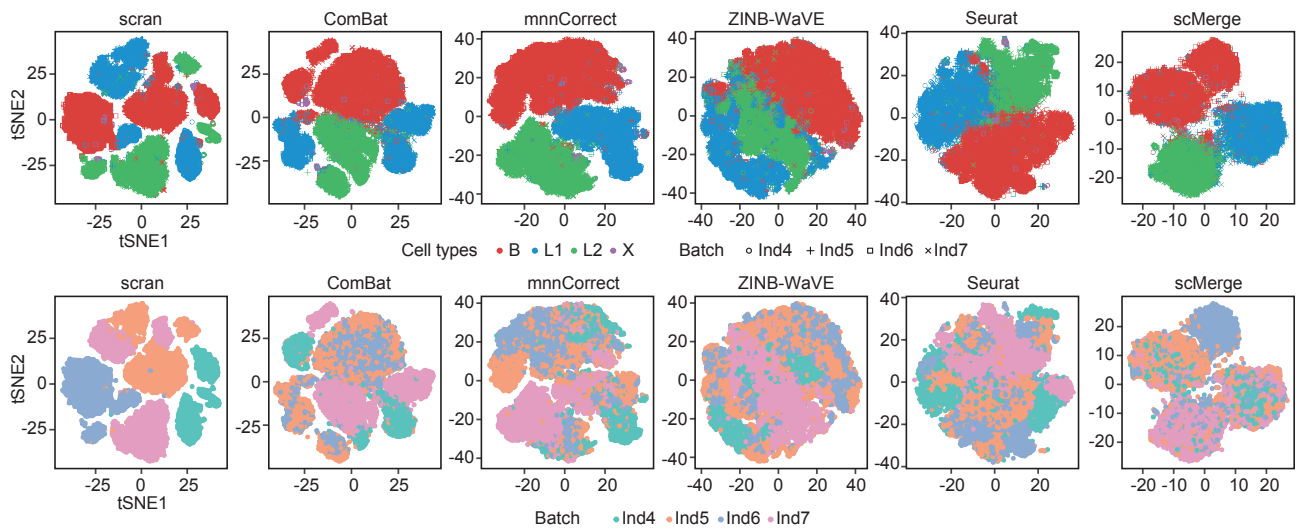


Fig. S7. A 2 by 6 panel of tSNE plots of the Breast Cancer data using the output from scran (logcounts), ComBat, mnnCorrect, ZINB-WaVE, Seurat, and scMerge (using scSEG as negative controls). The top row of the panel is color coded by cell types and the second row is color coded by the four individuals.

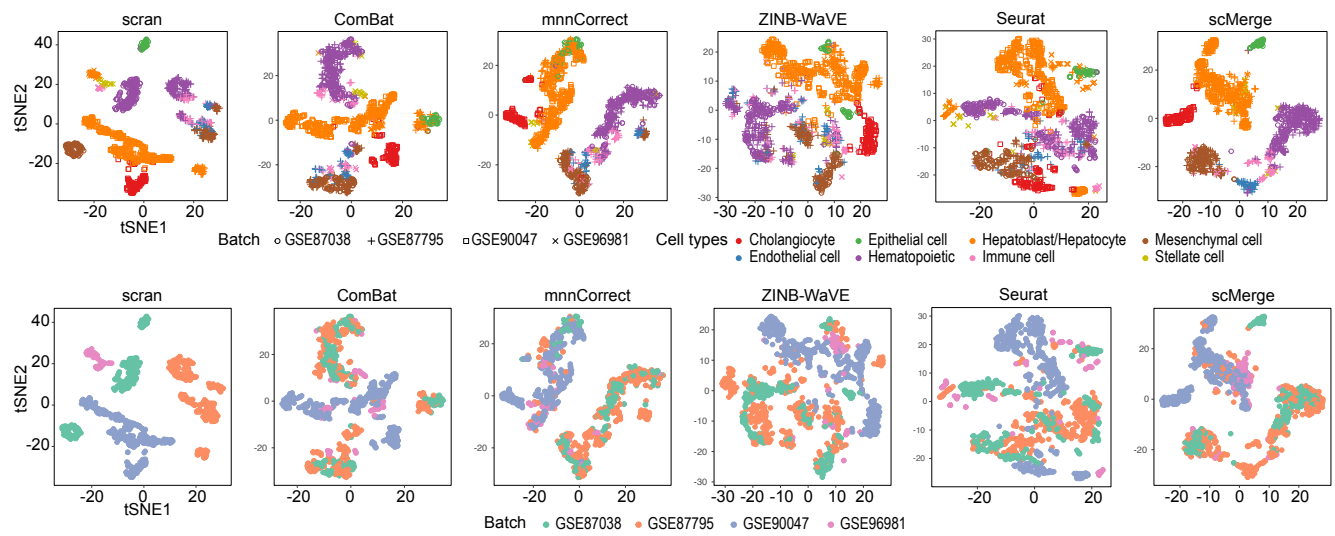


Fig. S8. A 2 by 6 panel of tSNE plots of the Liver data collection using the output from scrn (logcounts), ComBat, mnnCorrect, ZINB-WaVE, Seurat, and scMerge (using scSEG as negative controls). The top row of the panel is color coded by cell types and the second row is color coded by the four datasets.

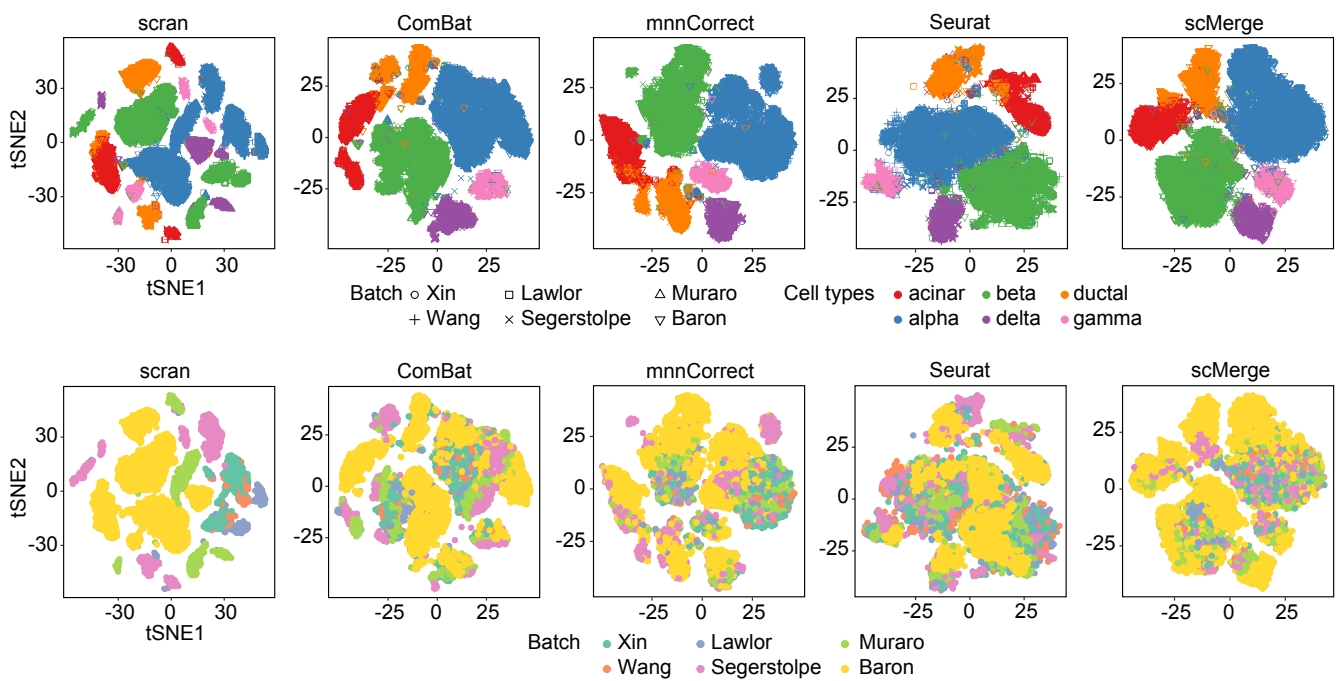


Fig. S9. A 2 by 6 panel of tSNE plots of the Olfactory data collection using the output from scran (logcounts), ComBat, mnnCorrect, ZINB-WaVE, Seurat, and scMerge (using scSEG as negative controls). The top row of the panel is color coded by cell types and the second row is color coded by the two datasets.

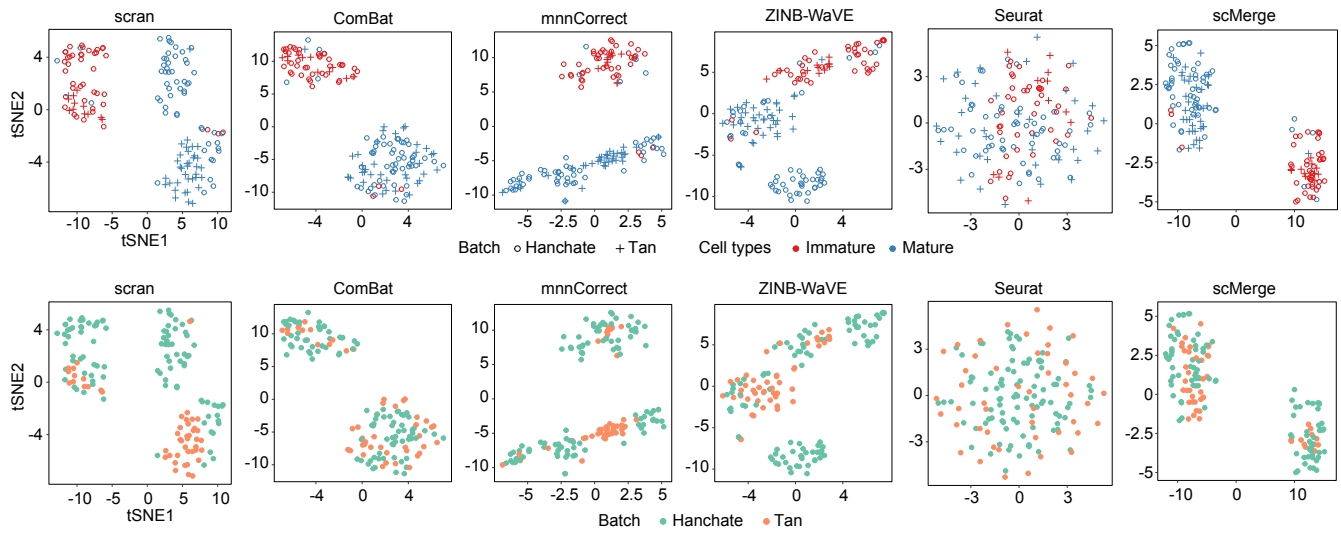


Fig. S10. A 2 by 6 panel of tSNE plots of all six Pancreas related datasets based on the output from scran (logcounts), ComBat, mnnCorrect, Seurat, and scMerge (using scSEG as negative controls). The top row of the panel is color coded by cell types and the second row is color coded by the six different datasets.

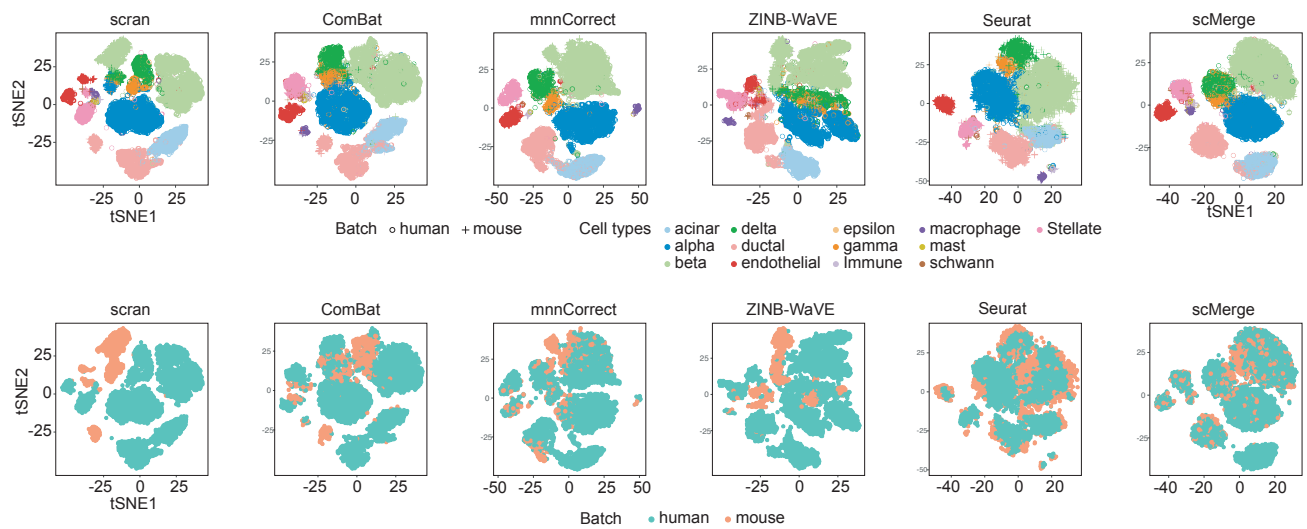


Fig. S11. A 2 by 6 panel of tSNE plots of the Pancreas Islet data collection using the output from scran (logcounts), ComBat, mnnCorrect, ZINB-WaVE, Seurat, and scMerge (using scSEG as negative controls). The top row of the panel color coded by cell types and the second row is color coded by the six datasets.

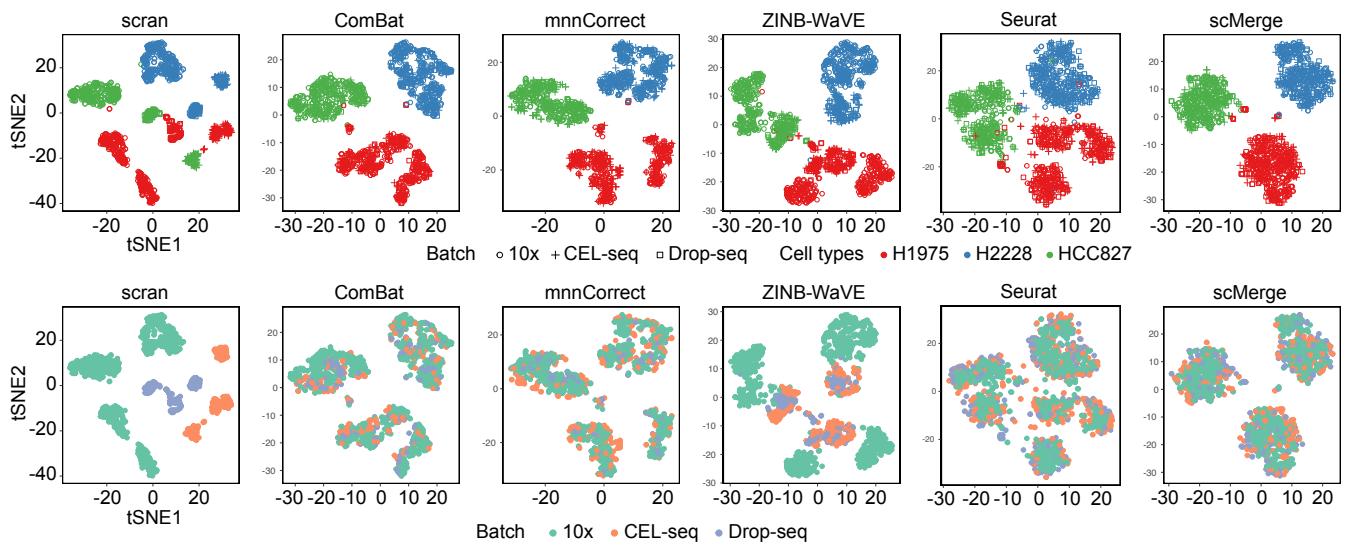


Fig. S12. A 2 by 6 panel of tSNE plots of the CellBench data using the output from scrn (logcounts), ComBat, mnnCorrect, ZINB-WaVE, Seurat, and scMerge (using scSEG as negative controls). The top row of the panel is color coded by cell lines and the second row is color coded by the three different platforms.

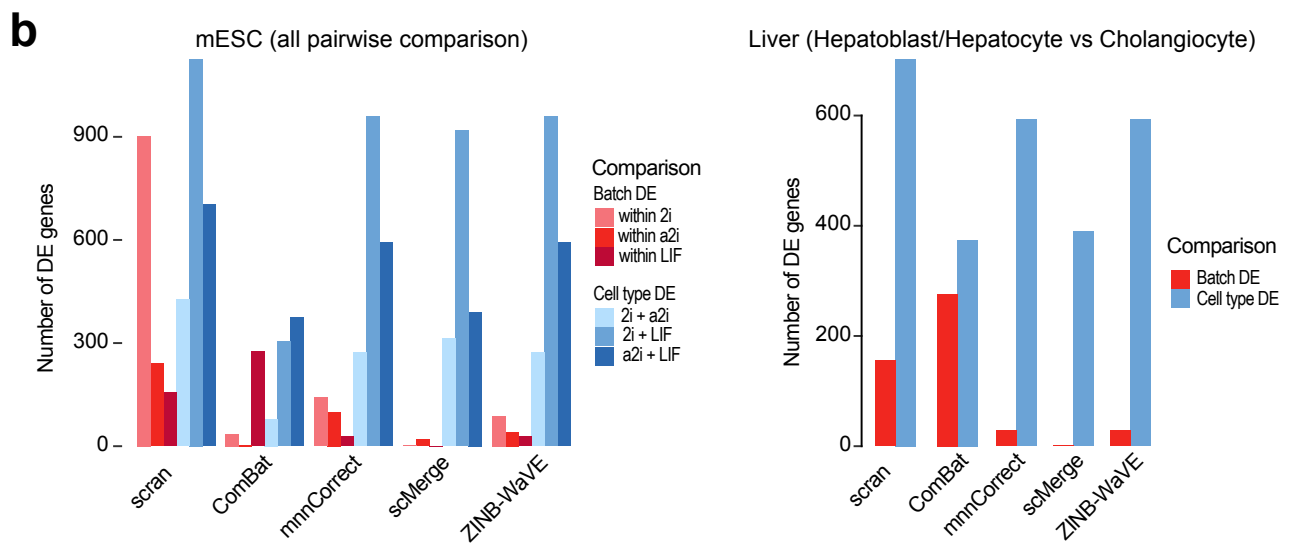
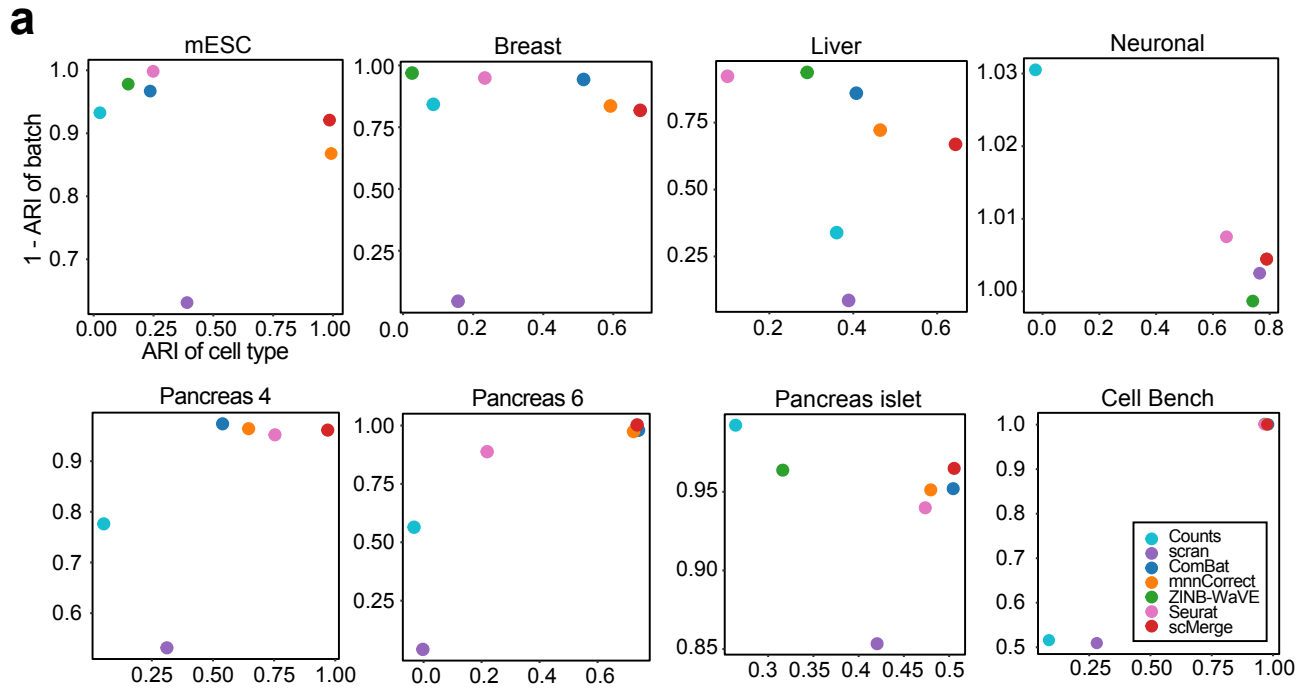


Fig. S13. (a) A 2 by 4 panel of scatter plots of ARI evaluation for no normalization, scran (logcounts), ZINB-WaVE, ComBat, mnnCorrect, Seurat, and scMerge (using scSEG as negative controls) of eight dataset collections (mESC dataset, breast). x-axes denote the ARI of cell types and y-axes denote the $1 - \text{ARI}$ of batch effects, where desirable outcomes are in the top-right hand corner. (b) A 1 by 2 panel of bar plots of differential expression results of mESC dataset (left panel) and liver dataset collection (right panel) on scran, ComBat, mnnCorrect, scMerge and ZINB-WaVE normalized data. The y-axis indicates the number of DE genes that are selected (adjusted p-value < 0.05 and $\log_{2}FC > 2$). Batch DE are selected by performing the DE analysis within the same cell type, while cell type DE are selected by performing the DE analysis between two different cell types.

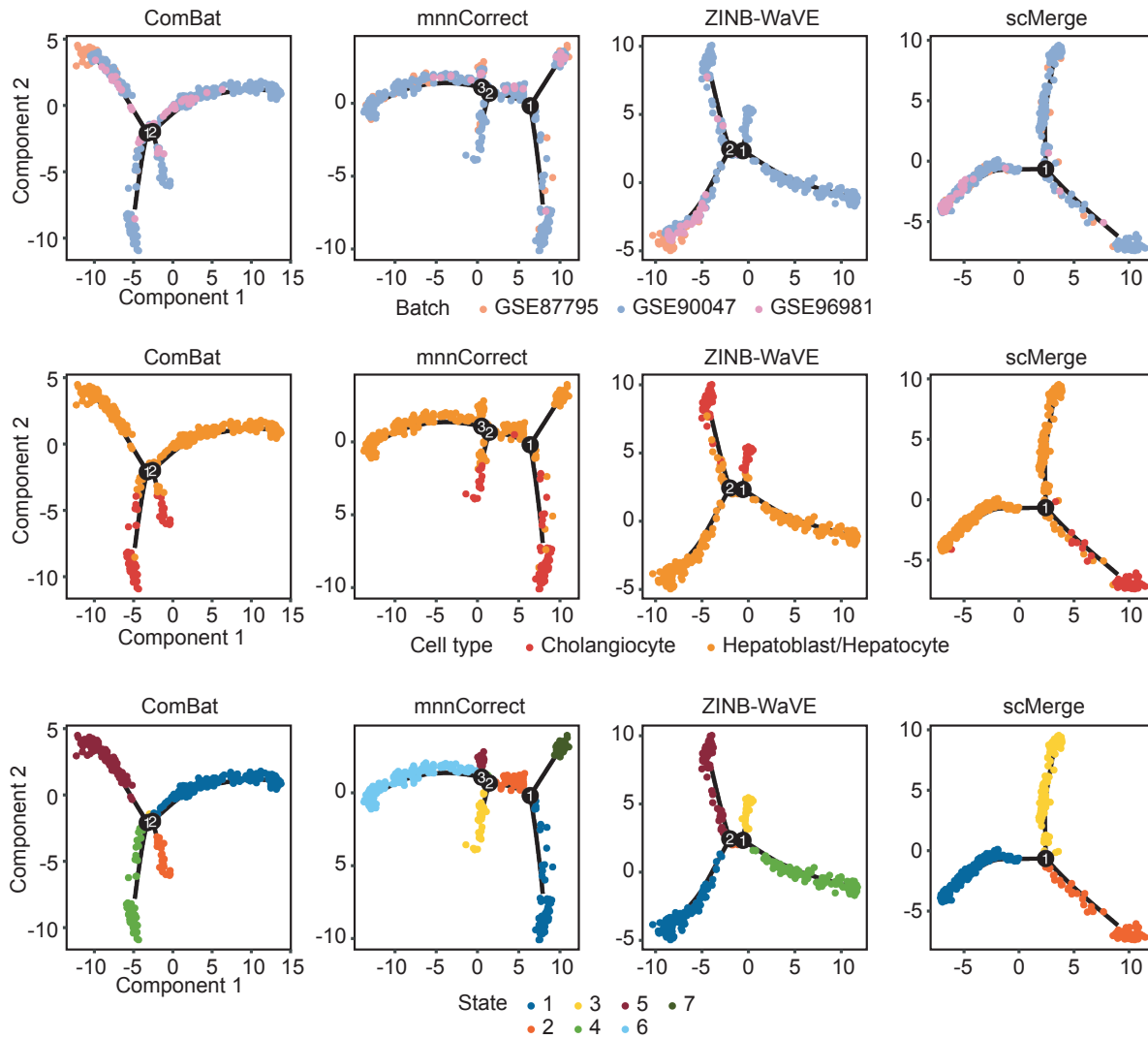


Fig. S14. A 3 by 4 panel of pseudotime trajectory from Monocle 2 with perturbed data demonstrating the stability of scMerge with output from ComBat, mnnCorrect, ZINB-WaVE and scMerge. The first row of the panel color coded by three datasets; the second row is color coded by the cell types and the third row is color coded by Monocle 2 states.

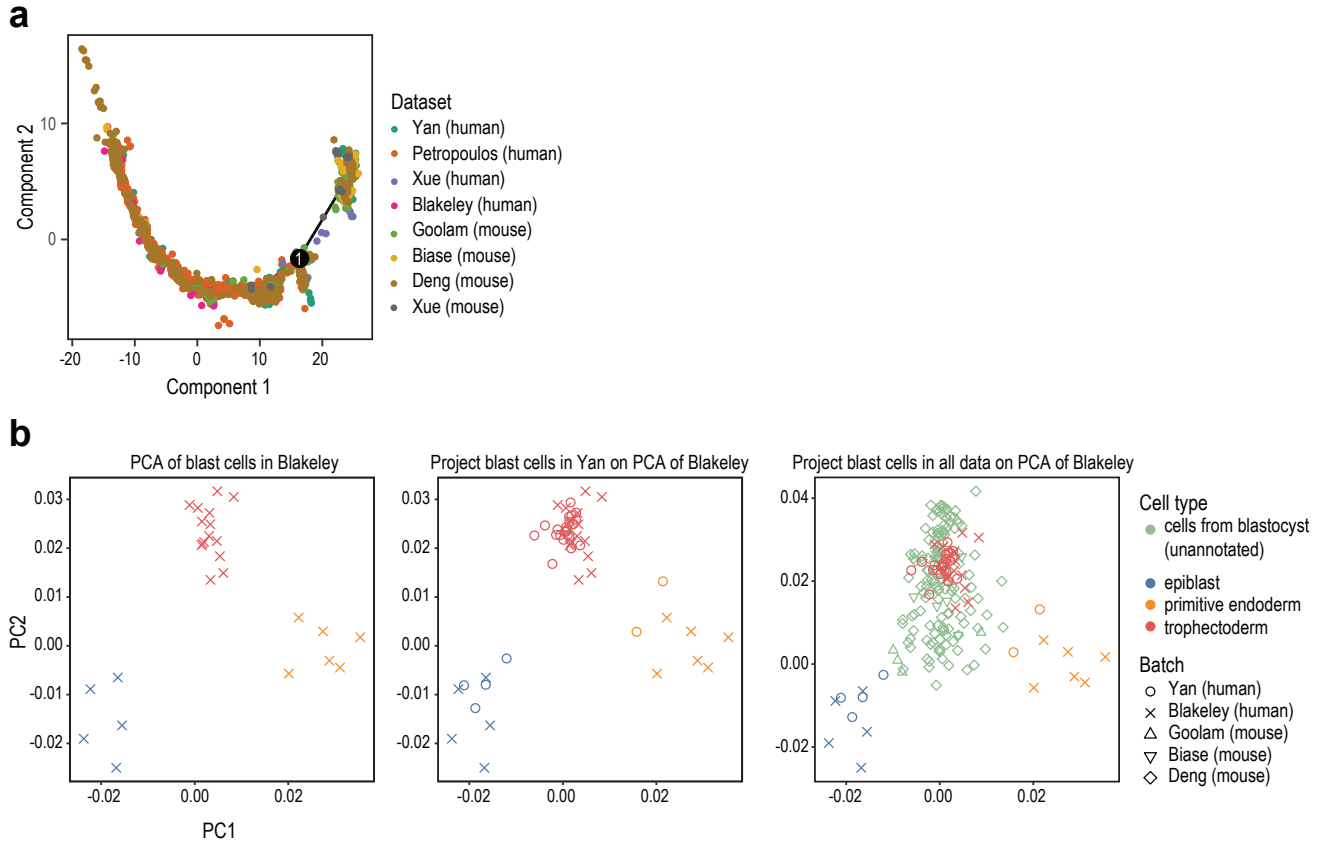


Fig. S15. (a) A pseudotime trajectory from Monocle 2 with all cells from ESC dataset collections, color coded by dataset. (b) A 1 by 3 panel of PCA plots of blast cells from ESC developmental data collections demonstrating scMerge effectively reproduce their cell type results, colored by the cell types identified from the original paper. The left panel is the PCA plot of blast cells from Blakeley et al. The medium panel is the PCA plot of blast cells from Blakeley et al. where blast cells from Yan et al. are projected. The right panel is the PCA plot of blast cells from Blakeley et al. where blast cells from mouse ESC datasets (Biase et al., Goolam et al. and Deng et al.) are projected.

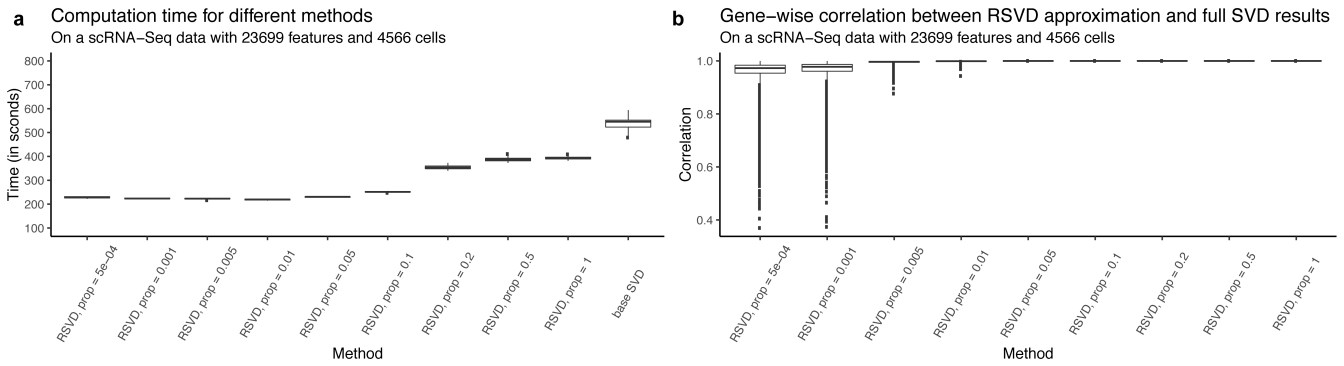


Fig. S16. (a) Computational time for different rsvd parameters with the Pancreas data collections ("Pancreas4"). This includes 23,699 features and 4566 cells. (b) Gene wise association based on Pearson correlation between rsvd approximation and full SVD calculation.

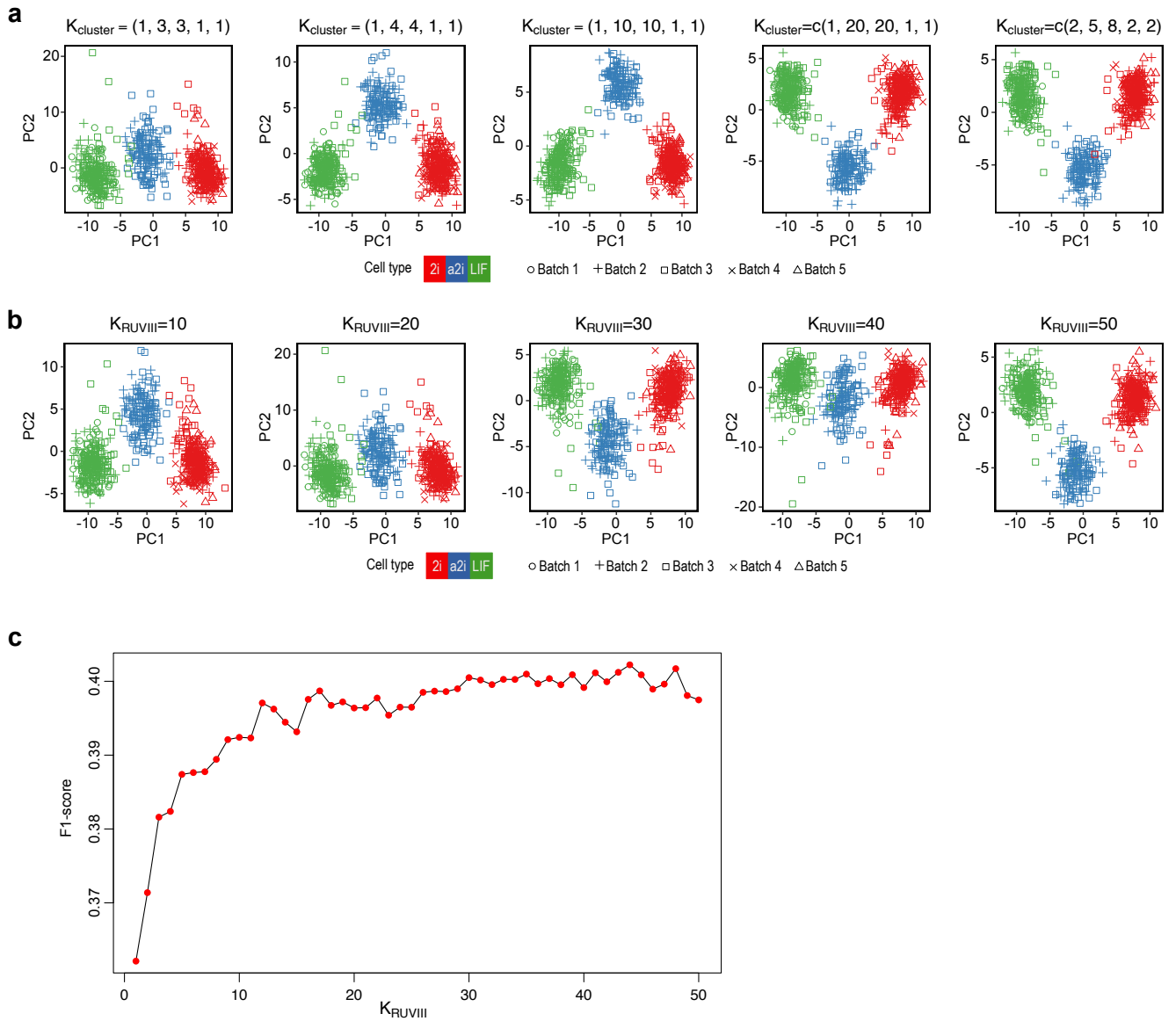


Fig. S17. (a) A 1 by 4 panel of PCA plots of mESC datasets using different $k_{cluster}$ settings. (b) A 1 by 4 panel of PCA plots of mESC datasets using different k_{RUVIII} settings ($k_{RUVIII} = 10, 20, 30, 40, 50$) (c) A scatter plot showing the performance of scMerge using different k_{RUVIII} from 1 to 50, evaluated by F1 score of Silhouette coefficient. The y-axis represents the F1-score, while the x-axis represents the k_{RUVIII} values.

Table S1. More detailed summary of datasets and data collections used in this study.

Supplementary Table 1

Type of merge	Name	ID	Author	DOI or URL	Protocol	Organism	Tissue	# of cell types	# of cells	# of batches
Within experiment	mESC	E-MTAB-2600	Kolodziejczyk	10.1016/j.stem.2015.09.011	SMARTer/C1	Mouse	Mouse ESC	3	704	5
	Breast	GSE113197	Nguyen	10.1038/s41467-018-04334-1	10x Chromium	Human	Breast cancer	3	24520	4
Across data experiments	Liver	GSE87795	Su	10.1186/s12864-017-4342-x	SMARTer/C1	Mouse	Liver	8	1236	NA
		GSE90047	Yang	10.1002/hep.29353	Smart-Seq2					
Across data experiments	Neuronal	GSE87038	Dong	10.1186/s13059-018-1416-2	STR1-seq	Mouse	Neuronal	2	145	NA
		GSE98981	Camp	10.1038/nature22796	SMARTer/C1					
Across data experiments	Pancreas	SRP065920	Tan	10.15252/msb.20156639	Smart-Seq2	Human	Pancreas	6	1773	NA
		GSE75413	Hanchate	10.1126/science.aad2456	STR1-seq					
Across data experiments	Pancreas	GSE81608	Xin	10.1016/j.cmet.2016.08.018	SMARTer/C1	Human	Pancreas	6	4566	NA
		GSE83139	Wang	10.2337/db16-0405	Smart-Seq					
Across data experiments	Pancreas	GSE86469	Lawlor	10.1101/gr.212720.116	SMARTer/C1	Human	Pancreas islets	13	8569	2 (human & mouse)
		E-MTAB-5061	Seegerstolpe	10.1016/j.cmet.2016.08.020	Smart-Seq2					
Across data experiments	CellBench	GSE83241	Muraro	10.1016/j.cels.2016.09.002	Cell-seq2	Human	Pancreas	6	1773	NA
		GSE84133	Baron	10.1016/j.cels.2016.08.011	inDrop	Human+ mouse	Pancreas islets	13	8569	2 (human & mouse)
Across platforms with significant depth difference	CellBench	cellBench		https://github.com/LuyiTian/CellBench_data	Cell-seq2, Drop-seq, 10x Chromium	Human	Adenocarcinoma cell lines	3	1401	3 per cell types
Across organisms	ESC	GSE45719	Deng	10.1126/science.1245316	Smart-Seq	Mouse	ESC	10+	2144	NA
		GSE57249	Biase	10.1101/gr.177725.114	SMARTer					
Across organisms	ESC	E-MTAB-3321	Goolam	10.1016/j.cell.2016.01.047	Smart-Seq2	Human + mouse	ESC	10+	2144	NA
		GSE44183	Xue	10.1038/nature12364	Tang et al., 2010*					
Across organisms	ESC	E-MTAB-3929	Petropoulos	10.1016/j.cell.2016.03.023	Smart-Seq2	human	ESC	10+	2144	NA
		GEO66507	Blakeley	10.1242/dev.123547	SMARTer					
Across organisms	ESC	GSE86552	Yan	10.1038/nrmb.2660	Than et al., 2010*	human	ESC	10+	2144	NA

Within experiment
 Across data experiments
 Across platforms with significant depth difference
 Across organisms
 * Tang et al., Nature Protocol, 2010 (DOI: 10.1038/nprot.2009.236)

Table S2. $F1_{sil}$ and $F1_{ARI}$ of all methods (counts, scran (logcounts), ComBat, mnnCorrect, ZINB-WaVE, Seurat, and scMerge) across all datasets.

Supplementary Table 2

Silhouette Coefficient	counts	scran	ComBat	mnnCorrect	ZINB-WaVE	Seurat	scMerge
mESC	0.52	0.56	0.58	0.68	0.57	0.52	0.69
Breast	0.42	0.27	0.52	0.55	0.53	0.53	0.59
Liver	0.35	0.26	0.53	0.52	0.51	0.52	0.53
Neuronal	0.56	0.54	0.60	0.61	0.56	0.53	0.61
Pancreas 4	0.44	0.41	0.56	0.59	NA	0.55	0.63
Pancreas 6	0.33	0.27	0.57	0.60	NA	0.51	0.61
Pancreas Islet	0.47	0.47	0.55	0.56	0.52	0.54	0.60
cellBench	0.47	0.39	0.64	0.63	0.65	0.54	0.65

ARI	counts	scran	ComBat	mnnCorrect	ZINB-WaVE	Seurat	scMerge
mESC	0.49	0.43	0.54	0.60	0.53	0.55	0.63
Breast	0.47	0.04	0.58	0.55	0.50	0.54	0.55
Liver	0.27	0.08	0.53	0.48	0.54	0.50	0.48
Neuronal	0.50	0.64	0.64	0.64	0.63	0.63	0.64
Pancreas 4	0.45	0.38	0.60	0.61	NA	0.61	0.65
Pancreas 6	0.36	0.04	0.63	0.62	NA	0.51	0.64
Pancreas Islet	0.56	0.53	0.58	0.58	0.56	0.57	0.59
cellBench	0.35	0.36	0.66	0.66	0.66	0.66	0.66

15 **Additional data table S1 (SupplementaryFile1.xlsx)**

16 Excel spreadsheet with six sheets listing scSEG and housekeeping genes derived from bulk microarray and bulk RNA-Seq,
17 for human and mouse each. Mouse bulk microarray and bulk RNA-Seq derived housekeeping gene lists are homologues of the
18 human gene lists given.

19 **Additional data table S2 (SupplementaryFile2.xlsx)**

20 Excel spreadsheet with pseudotime estimation for all cells from ESC data collections.